Design and Experimental Validation of Heat Exchangers Equipment for 2 kW Model of Binary Cycle Power Plant

Bambang Teguh P[1]., Himawan S.[1], Suyanto, Taufan S.[2], MD Trisno[3]

[1]BTMP-BPPT, 230 building, Puspiptek, Serpong – Tangerang, 15314, Indonesia

[2]PTKKE, BPPT building, Tour II, Floor 20, Jl. MH. Thamrin, No. 8. Jakarta

[3]Lecturer in Mech. Engineering Dept.- ISTN-Jakarta

prasetyo@doctor.com, bambang@btmp-bppt.net

ABSTRACT

Currently, 100% of brine at direct-steam geothermal power plant is injected into injection wells. Injected brine generally has a temperature higher than 100°C and mass flow rate around hundred of ton/hour. The rapid estimation showed the content of rejected energy is around hundred millions of watts. Binary cycle plant may be advantageous technology to recover this energy waste. In order to study the implementation above technology, BPPT has developed the 2 kW model of binary cycle power plant using the thermal energy of brine. In this plant, thermal energy of brine is transferred via a heat exchanger to working fluid for use in a fairly conventional Rankine cycle. The power cycle consists of an evaporator, a turbine-generator, a condenser, and feed pump. Other equipment is cooling tower to serve the condenser cooling water. The working fluid used in this plant is n-pentane to achieve a good thermodynamic match to the particular characteristics of brine, especially brine temperature. This paper presents the design and testing of heat exchangers equipments and n-pentane turbine of this binary cycle plant model. From design analysis the heat exchanger equipment to be used are 56.31 kW shell and tube evaporator, 53.68 kW shell and tube condenser. The turbine design is single-stage impulse turbine with five convergent nozzles, 382.3 mm rotor diameter, 60 blades, 16.5 mm height of blade, and 10 mm width of blade. This turbine is designed to operate at 3000 rpm and 65.6% turbine efficiency. Experimental result showed that the system has successfully produced 1.2 kWe. There is 8.5% different in efficiency lower than design condition The method of design and the result of experiment will be discussed in this paper.

1. INTRODUCTION

1.1 Thermal Waste of Direct Steam Plant

Indonesia has the largest geothermal resources in the world, with a potential of 40% in the world, around 27,000 MW. Indonesia has been focusing on the development of high enthalpy geothermal resources. Geothermal power plants have been operated around 1052 MW in Indonesia that are direct-steam plants type. 100% of separated brine from these plants is reinjected into injection wells. The reinjected brine generally has a temperature higher than 100°C and mass flow rate of hundred ton per hour. Therefore the thermal energy rejected is around hundred million watts. An example for 1×110 MW direct-steam geothermal power plant existing in West Java, rejected brine is around 270 ton/hr at 180°C and 11.0 bar (abs), containing thermal energy around 57.23 MW.

This thermal energy of the brine can be recovered by transferring via a heat exchanger to working fluid for use in other process. In this case, depending on silica content in the brine, minimum temperature drop of brine permitted in heat exchanger is limited by silica scaling formation

Assuming the permitted temperature drop of this brine in heat exchanger is until 140°C, then the thermal energy that can be recovered is about 13 MW thermal.

In the era of energy crisis, this energy waste is very important to be concerned to increase energy saving and efficiency. On the other hand, in Indonesia there are a lot of low-to-medium enthalpy resources which can also be utilized for electricity generation, but they are not developed optimally yet.

1.2 Binary Cycle Plant

Binary cycle plant is an advantageous technology for recovering the energy waste or unusable energy especially at low geo-fluid temperatures (150°C), or geo-fluids with high corrosion and scaling potential. In a binary cycle plant, thermal energy of brine or geo-fluid is transferred through a heat exchanger to working fluid for using in a fairly conventional Rankine cycle. A flow diagram for typical basic binary plant is shown in Figure 1.
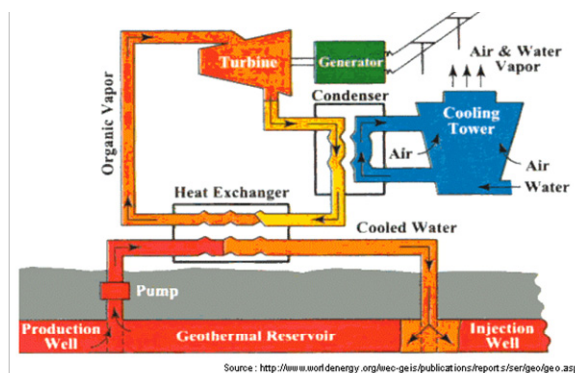

Figure 1. Schematic of binary cycle geothermal power-plant Source: http://www.worldenergy.org

The power cycle consists of heat exchangers (pre-heater and evaporator), a set of control valves, a turbine-generator set, a condenser, and feed pump. Either water or air may be used for cooling depending on the applied cooling systems. If the wet cooling system is applied, an independent source of make-up water must be found. Owing to chemical impurities, the waste brine is not suitable for cooling tower make-up.

The engineering designer must consider a wide range of candidate working fluids for the power cycle. For making the selection, one tries to achieve a good thermodynamic match to the particular characteristics of the geo-fluid, especially the geo-fluid temperature. Among the important properties of candidate working fluids are: critical temperature and pressure, saturation properties (including whether the fluid exhibits retrograde condensation, thermal stability, flammability, toxicity, ozone depletion potential, heat transfer coefficients, speed of sound at turbine exhaust condition, and cost. Hydrocarbons such as isobutane, isopentane, and propane are good candidate working fluids as are certain refrigerants.

The optimal fluid will give high utilization efficiency together with safe and economical operation. Binary plants lend themselves very well to modular packages in the power range of 1 to 3 MW per unit.

In order to study the implementation of binary plant technology, BPPT has developed the 2 kW model of binary cycle power plant using thermal energy of brine. A diagram of this model is shown in Figure 2. The power cycle consists of an evaporator, a turbine-generator, a condenser, and feed pump. Other equipment is a cooling tower to serve the condenser cooling water. Thermal energy of brine is transferred trough a heat exchanger (evaporator) to working fluid. The working fluid of the plant is n-pentane. The paper presents the design and testing of this binary cycle plant model. Experimental validation of this plant was conducted using a small extraction of brine at Wayang Windu geothermal power plant.
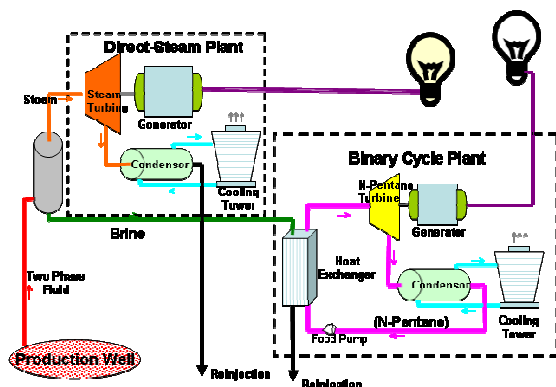

Figure 2. Diagram for binary plant using brine as thermal energy resources. Source: Bambang T. Prasetyo (2008)

1.3 Heat Exchangers

Many types of heat exchanger (plates, tubular, etc) can be used as evaporator and condenser. But in this study, shell and tube type is chosen because its has some advantages, for example: very simple geometry, well-established design procedure, can be constructed from a wide range of materials, uses well-established fabrication techniques, easily cleaned, and technicians were familiarized with this technology.

Essentially, a shell and tube exchanger consists of a bundle of tubes enclosed in a cylindrical shell. The ends of the tubes are fitted into tube sheets, which separate the shell-side and tube-side fluids. Baffles are provided in the shell to direct the fluid flow and support the tubes. The assembly of baffles and tubes is held together by support rods and spacers. An example of shell and tube heat exchanger assembly is shown in Figure 3.

Figure 3. Schematic of shell and tube heat exchanger, Source; www.mdtofis.com

The principle types of shell and tube exchanger classified by TEMA Standards are shown in Figure 4.

Figure 4. Type of shell and tube heat exchanger, TEMA (1998).

The classical method of thermal design for heat exchanger is the Logarithmic Mean Temperature Difference (LMTD) method. Application of this method is limited because in the correlation used to predict heat transfer coefficients, the physical properties (density, viscosity, thermal conductivity, etc) are evaluated at the mean stream temperature and assumed constant along the length of heat exchanger. This approximation is satisfactory when the fluid temperature change along of heat exchanger is small.

When the temperature change is large, this approach can cause a significant error. In this circumstance, it will be necessary to divide temperature – enthalpy of fluid into some segments along the length of heat exchanger, and evaluate heat transfer coefficient and required surface area for every segment, R. K. Sinott (1998). This method is known as the Temperature-Enthalpy (T-H) diagram method. H. J. Brackenbury (1993) has developed software to design heat exchangers by using the method wherein the solution is based on heat transfer process changes of the working fluid.

T-H method is a LMTD method applied at each segment along the entire heat exchanger. The logic calculation using T-H method to determine heat transfer area is first,

calculation of the T-H profile and second calculation of the heat transfer area.

1.3.1 Calculation of T-H Profile

- Single-tube Pass Exchanger

Figure 5 illustrates the operation of a single pass counter-flow exchanger with flow-rate $\dot{m}_s$ on the shell side and $\dot{m}_t$ on the tube side. A heat balance over area A of the exchanger gives:

$$\left(H_s - H_{s,out}\right)\dot{m}_s = \left(H_t - H_{t,in}\right)\dot{m}_t \qquad (1)$$
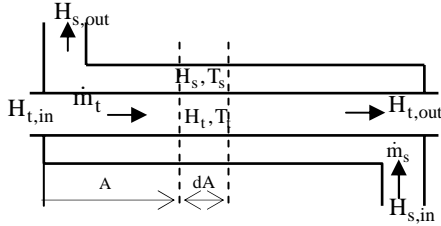

Figure 5. Schematic diagram of a counter-flow, single pass exchanger

Where H_s and H_t are respectively the shell-side and tube-side specific enthalpies and the subscript 'in' and 'out' refer respectively to the inlet and outlet of the fluid streams. Hence, the tube-side specific enthalpy can be explicitly expressed in the terms of the shell-side enthalpy as follows:

$$H_t - H_{t,in} = \frac{\dot{m}_s}{\dot{m}_t}\left(H_s - H_{s,out}\right) \qquad (2)$$

$$H_t - H_{t,out} = -\frac{\dot{m}_s}{\dot{m}_t}\left(H_{s,in} - H_s\right) \qquad (3)$$

where equation (3) is determined from equation (2) using the following heat balance over the whole exchanger.

$$\dot{Q}_T = \left(H_{s,in} - H_{s,out}\right)\dot{m}_s = \left(H_{t,out} - H_{t,in}\right)\dot{m}_t \qquad (4)$$

It is assumed here that the relationship between the temperature and the specific enthalpy is known for each stream. The shell-side temperature, T_s, can therefore be plotted as a function of the shell-side specific enthalpy as illustrated on Figure 6. Using equation (2) or (3) and the tube-side T-H curve, the tube-side temperature, T_t, can also be plotted against H_s as shown in Figure 6. The temperature difference T_s-T_t can therefore be obtained for any value of H_s. It is worth nothing that Figure 6 is independent of heat transfer coefficient and hence of the detailed geometry. In a design, therefore, the diagrams need only be obtained once for all single-pass exchangers.
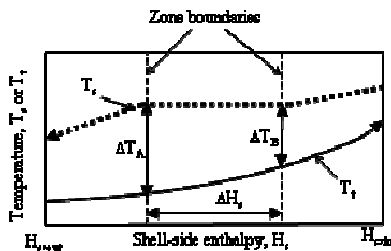

Figure 6. Illustration of the temperature-enthalpy diagram for single pass counter-flow exchanger

- Two-tube Pass Exchanger

Figure 7 illustrates the operation of two-tube pass exchanger in which the shell-side flow is counter-current to the first pass and co-current to the second.
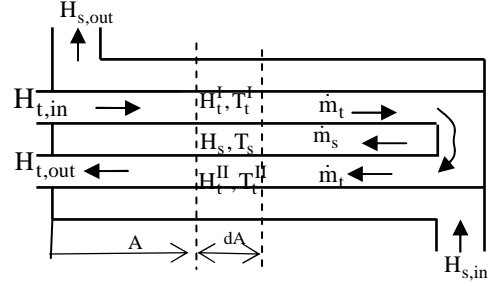

Figure 7. Schematic diagram of a two-tube pass exchanger

A heat balance over area A of exchanger give;

$$\left(H_s - H_{s,out}\right)\dot{m}_s = \left(H_t^I - H_{t,in} + H_{t,out} - H_t^{II}\right)\dot{m}_t \qquad (5)$$

where H_t^I and H_t^{II} are the specific enthalpies in pass I and II respectively. Combining this with the overall balance for the exchanger (equation 4) gives;

$$H_s = H_{s,in} - \frac{\dot{m}_t}{\dot{m}_s}\left(H_t^{II} - H_t^I\right) \qquad (6)$$

An incremental heat balance over dA for pass I gives;

$$\dot{m}_t dH_t^I = U^I\left(T_s - T_t^I\right)\frac{dA}{2} \qquad (7)$$

where it is assumed that half the area is in each pass. U^I is the overall coefficient and T_t^I the temperature for pass I. Similarly for pass II ;

$$\dot{m}_t dH_t^{II} = U^{II}\left(T_s - T_t^{II}\right)\frac{dA}{2} \qquad (8)$$

Dividing equation (7) by equation (8) gives;

$$\frac{dH_t^{II}}{dH_t^I} = -\frac{U^{II}}{U^I}\frac{\left(T_s - T_t^{II}\right)}{\left(T_s - T_t^I\right)} \qquad (9)$$

Starting with $H_t^I = H_{t,in}$ when $H_t^{II} = H_{t,out}$, this equation may be integrated numerically over the exchanger by using the following other relationships;

a. equation (6) relating the shell-side to the tube-side enthalpies,
b. the T-H curves for each stream, and
c. relationships expressing the overall coefficient U as a function of H_t, H_s and T_s-T_t .

Integration is stopped when $H_t^I = H_t^{II}$ and the results may be plotted on a T-H diagram as illustrated in Figure 8
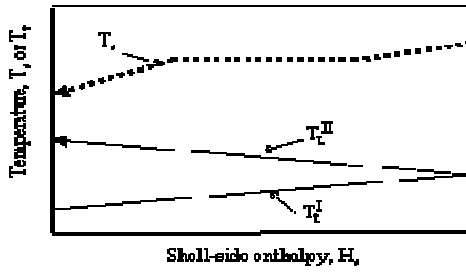
Figure 8. Illustration of the T-H diagram for a two-tube pass exchanger

The integration can be greatly simplified if it is assumed that U^I is equal to U^{II} at every position along the tube length although they can still both vary along the length. For this case, equation (9) becomes;

$$\frac{dH_t^{II}}{dH_t^I} = -\frac{\left(T_s - T_t^{II}\right)}{\left(T_s - T_t^I\right)} \qquad (10)$$

This equation can be integrated as before but data on the overall coefficients are not required. Since only the coefficients are geometry-dependent, the T-H diagram is determined only once for all two-tube pass exchangers. This simplification is used in design mode to give considerable savings in run time.

- Multi-tube Pass Exchangers

Repeating the above analysis for multi-pass exchanger with an event number of passes gives the following relationships between the shell-side and tube-side conditions;

$$H_s = H_{s,in} + \frac{\dot{m}_t}{\dot{m}_s}\left(H_t^I - H_t^{II}.... - H_t^N\right) \qquad (11)$$

and

$$\frac{dH_t^{II}}{dH_t^I} = -\frac{U^{II}}{U^I}\frac{\left(T_s - T_t^{II}\right)}{\left(T_s - T_t^I\right)} \qquad (12.a)$$

$$\frac{dH_t^{III}}{dH_t^I} = -\frac{U^{III}}{U^I}\frac{\left(T_s - T_t^{III}\right)}{\left(T_s - T_t^I\right)} \qquad (12.b)$$

$$\frac{dH_t^{(N)}}{dH_t^I} = -\frac{U^{(N)}}{U^I}\frac{\left(T_s - T_t^N\right)}{\left(T_s - T_t^I\right)} \qquad (12.c)$$

where N is the number of passes

As with the two-pass exchanger, these equation may be integrated through the exchanger except that, now, all the boundary conditions are not known in advance. The enthalpies (and temperatures) of the tube-side fluid as it leaves the second pass and enters the third and as it leaves the fourth and enters the fifth et., are unknown. An iteration is therefore required to determine thew values of the avbove interpass enthalpies which cause $H_t^I = H_t^{II}$, $H_t^{III} = H_t^{IV}$ etc, when $H_s = H_{s,in}$

1.3.2. Calculation of Required Heat Transfer Area

The rate of heat transfer through a small area of heat exchanger dA is given by;

$$\dot{m}_s dH_s = U\Delta T dA \qquad (13)$$

where $\dot{m}_s$ is the shell-side mass flow-rate, dH_s is the change in shell side enthalpy across the small area dA, U is the local overall heat transfer coefficient and ΔT is the local temperature difference.

The area required for whole exchanger must be calculated and, hence, equation (13) is rearranged and integrated as follows;

$$A_{req} = \dot{m}_s \int_{H_{s,in}}^{H_{s,out}} \frac{dH_s}{U\Delta T} \qquad (14)$$

The T-H profile is used to solve equation (12) numerically. The curve is split into a number of zones, where equation (13) is solved for each zone and the zonal areas summed to get A_{req}. (U_i and ΔT_i are now the average overall coefficient and temperature difference across the zone). The curve gives the shell-side and tube-side temperatures at each end of the zone from which ΔT_i can be calculated; the size of the equipment will dictate velocities and hence heat transfer coefficients

$$A_i = \dot{m}_s\left(\frac{dH_s}{U\Delta T}\right)_i \qquad (15)$$

- Evaluation of Zonal Temperature Difference

When dividing the T-H profile into zones, the zone boundaries are chosen such that T_s and T_t may be considered as varying linearly with H over each zone, hence the LMTD may be used to evaluate ΔT_i. LMTD is given by,

$$\Delta T_i = \frac{\left(T_s - T_t\right)_a - \left(T_s - T_t\right)_b}{\ln\frac{\left(T_s - T_t\right)_a}{\left(T_s - T_t\right)_b}} = \frac{\Delta T_a - \Delta T_b}{\ln\left(\frac{\Delta T_a}{\Delta T_b}\right)} \qquad (16)$$

where $\left(T_s - T_t\right)_a$ and $\left(T_s - T_t\right)_b$ are the temperature differences at each end of the zone.

For multi-pass exchangers $\left(T_s - T_t\right)_a$ and $\left(T_s - T_t\right)_b$ are replaced by the differences between the shell-side temperature and the average tube-side temperature. In the two-tube pass case these are evaluated using,

$$T_s - \overline{T}_t = \frac{U^I\left(T_s - T_t^I\right) - U^{II}\left(T_s - T_t^{II}\right)}{U^I + U^{II}} \qquad (17)$$

where U^I and U^{II} are the local overall coefficients and T_t^I and T_t^I the tube-side temperatures in passes 1 and 2 respectively at the relevant zone boundary.

- Evaluation of zonal overall heat transfer coefficient U

Local overall heat transfer coefficient at each zone boundary referred to the tube outside diameter is

$$U = \frac{1}{\frac{1}{h_s} + \frac{1}{h_{fs}} + \frac{d_o\ln(d_o/d_i)}{2k_w} + \frac{d_o}{d_ih_{ft}} + \frac{d_o}{d_ih_t}} \qquad (18)$$

where h_s, h_t; are the local shell-side and tube-side heat transfer coefficients respectively, h_{fs}, h_{ft}; are the shell-side and tube-side fouling coefficients, d_o, d_i; are the tube outer

and inner diameters respectively, and k_w; is the tube wall thermal.

The local overall coefficients are average across the zone to give the zonal overall heat transfer coefficient using :

$$U_i = \frac{1}{2}\left(U_a + U_b\right) \qquad (19)$$

For multi-pass exchangers U_a and U_b are replaced by coefficients which have been average between the pass. In the two pass case this averaging between passes is given :

$$\overline{U} = \frac{1}{2}\left(U^I + U^{II}\right) \qquad (20)$$

1.4 N-Pentane Turbine

Turbine designing for this system is based on a simple impulse turbine calculation with single stage of velocity and pressure. The schematic diagram of turbine design is shown in Figure 9, P. Shlyakhin (s.a.).
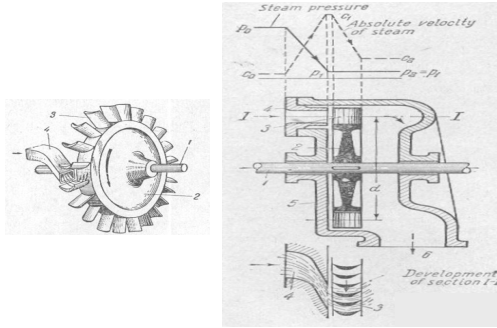

Figure 9. Diagram for single stage impulse turbine, 1 Shaft, 2 Disc, 3 Moving blades, 4 Nozzle, 5 Stator, 6 Exhaust pipe

The main components of turbine are shaft, disc, moving blade, nozzle, stator and exhaust pipe. Depending to thermodynamic and physical properties of n-pentane vapor, a convergent nozzle is used with a consideration that the maximum velocity is equal to critical velocity in the throat. Referring to this configuration, the transformation of energy in the moving blades is illustrated in the Figure 10, with c_1 is an absolute velocity of working fluid into the blade passages, α_1 is angle of entry, u is rotation velocity of turbine disc, w_1 is relative velocity of entry of working fluid at an angle β_1, w_2 is relative velocity of working fluid leaves the blades at an angle β_2, and c_2 is absolute velocity of working fluid leaves the blades at an angle α_2.

Therefore, if $\dot{m}$ is mass flowrate of working fluid, the thermal power of working fluid transfering to the moving blades can be expressed as:

$$P = \dot{m}\,u\left(c_1\cos\alpha_1 - c_2\cos\alpha_2\right) \qquad (21)$$

N-pentane is a flammable fluid. Therefore the most important part in the design is a seal. Instantly, for reasoning to the simplicity of design, we use a stuffing box as a seal between shaft and stator.
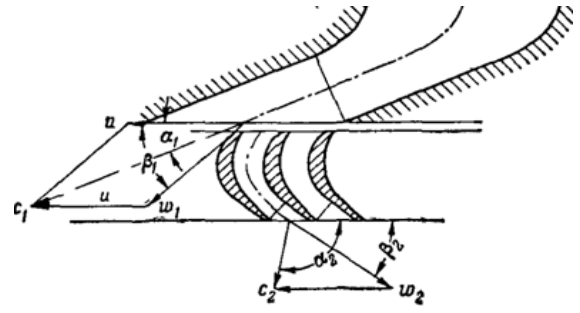

Figure 10. Variation of velocity of fluid on moving blades of an impulse stage, Source: P. Shlyakhin (s.a.).

Referring to P.Shlyakhin (s.a.), the step of turbine design calculation is as follows:

- Theoretical enthalpy drop in nozzle (Δh_t)

Schematic diagram of steam flow in the nozzle is shown in Figure 11:

$$\Delta h_t = h_0 - h_1 \qquad (22)$$

where h_0 and h_1 are specific enthalpy of steam inlet and outlet nozzle respectively.

- Theoretical velocity of steam outlet nozzle (c_{1t})

Neglecting the potential and kinetic energy of steam flow inlet nozzle and assuming the energy losses of flow inside nozzle is relatively small, the velocity of steam outlet nozzle is:

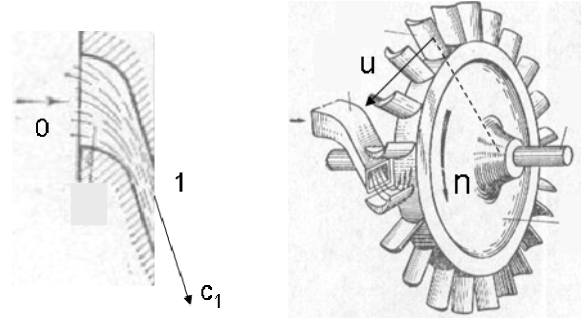$$c_{1t} = \sqrt{2\,\Delta h_t} \qquad (23)$$

Figure 11. Flow in the nozzle   Figure 12. Turbine Rotor

where F_1 is velocity coefficient giving around 0.92.

- Rotor rotation velocity (u)

The rotor of the turbine is shown schematically in Figure 12, and the relation of efficiency as a function of u/c_1 for *single-stage impulse turbine* is shown in Figure 13. The optimum of u/c_1 is around 0.4 , therefore, in this study the rotation velocity of rotor is taken $u = 0,4\,c_1$

2. METHODOLOGY

2.1 Design of System

With certain consideration, design of 2kW binary cycle power plant is shown in Figure 11, Bambang T. Prasetyo (2006).
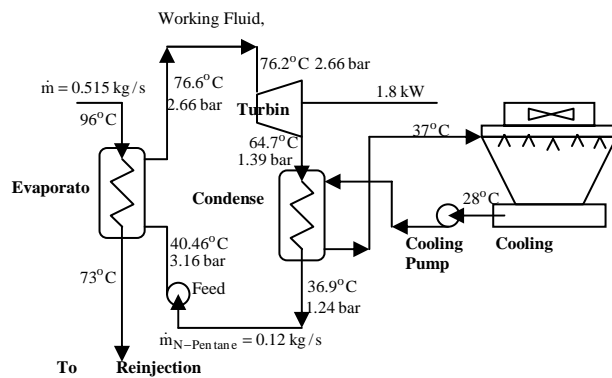
Figure 11. Diagram for binary plant and design parameters.

2.2 Design of Heat Exchangers

Heat exchangers in the 2 kW binary cycle geothermal power plant consist of an evaporator, a condenser and cooling tower. Wet cooling tower was chosen to serve the condenser cooling water. Evaporator and condenser are shell and tube type. This type is chosen because its have some of advantages. The most important consideration is its can be easily designed and manufactured locally.

In this project study, for sizing of evaporator and condenser, the T-H diagram method is used for thermal design and TEMA (1998), standard for mechanical design. The design of a shell and tube heat exchanger consists of three step activities i.e. thermal design, mechanical design, and checking. In the thermal design, the process conditions and limitations are inserted to the program along with the preferences to meet process requirement and engineering designer interests. In this step, the configuration is set and the performance of the exchanger is calculated. The exchanger configuration is then evaluated to satisfy mechanical limitations. Then the corrected configuration is examined again to evaluate the performance of the heat exchanger.

According to the process data as above mentioned in Figure 3, the design calculation of evaporator and condenser was done using the T-H method. The evaporator is a shell and tube BFM type wherein brine flows in the tube side and n–pentane is vaporized in the shell side. The evaporator has shell diameter of 339.8 mm and tube length of 1500 mm. The total duty is 56.31 kW. The condenser is also shell and tube type, but regarding to the function, the chosen type is BXM wherein cooling water flows in the tube side and n-pentane condenses in the shell side. The condenser has shell diameter of 340 mm and tube length of 1500 mm. The total duty is 53.68 kW

2.2 Design of N-Pentane Turbine

Referring to design parameters, the n-pentane turbine was designed with an enthalpy drop of 12.5 kJ/kg and flow rate of 0.139 kg/s. The estimated turbine thermal power is around 1.73 kW. The rotation velocity of shaft is designed to be 3000 rpm

3. RESULT AND DISCUSSION

3.1 Heat Exchangers

The main dimensions of evaporator and condenser are presented in Tables 1 and 2. The manufacturing of heat exchanger component assembly is shown in Figure 12 and 13, Bambang T. Prasetyo (2006).

Table 1. Dimensions of n-pentane evaporator

Tube	
Fluid flow	Hot Brine
Number of tube	180
Number of pass	2
OD/ID (mm)	15.88/ 13.88
Arangement	30°
Pitch tube (mm)	21
Length (mm)	1500
Material	Carbon steel
Shell	
Fluid flow	n-pentane
ID (mm)	339.8
Material	Carbon steel
Baffle	
Type	Single segmental
Cut	20%
Number	12
Midspace (mm)	95
Endspace (mm)	197
Material	Carbon steel

Table 2. Dimensions of n-pentane condenser

Tube	
Fluid	Cooling water
Number of tube	180
Number of pass	4
OD/ID (mm)	15.88/13.88
Arangement	30°
Pitch tube (mm)	20
Length (mm)	1500
Material	Carbon steel
Shell	
Fluid	n-pentane
ID (mm)	340
Material	Carbon steel
Baffle	
Type	Support baffle
Cut	
Number	
Midspace (mm)	
Endspace (mm)	
Material	Carbon steel

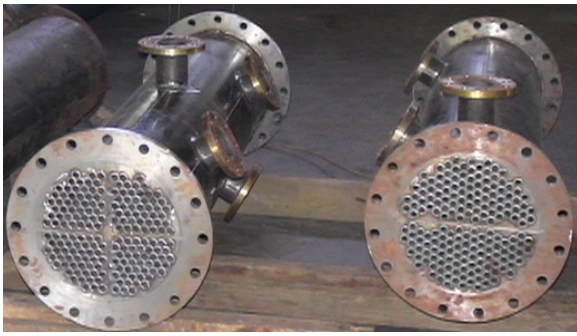**Figure 12. Tube bundle of evaporator**

Figure 13. Assembly of evaporator and condenser

3.2 n-Pentane Turbine

The result of design calculation is shown at Figure 14, and the detailed dimensions are showed in Table 3, Bambang T. Prasetyo (2006).

Figure 14. Photo of parts and assembly of 2 kW n-pentane turbine

Table 3. Dimensions of n-pentane turbine parts

Parts	Dimension		
Nozzle	number		5.0
	height	mm	10.0
	widht	mm	5.0
	angle α_1(o)	(o)	14.5
Rotor	pitch diameter	mm	382.3
	shaft diameter	mm	33.0
Blades	number		60.0
	Height	mm	12/16.6
	width	mm	10.0
	angle β_1	(o)	23.8
	angle β_2	(o)	16.8
	radius of curvature R	mm	13.8
	Pitch	mm	20

3.3 Experiments

Performance test of the 2 kW binary cycle geothermal powerplant was carried out at Wayang Windu Geothermal Power Plant facility. The heat source for running the model came from hot brine tapped from an injection well pipeline. The assembly of all equipment on site is shown in Figure 15.

Some measurements were established at the points as shown in the Figure 16 to analyze the performance of the binary cycle plant. The results of the experiment can be summarized in Table 4.

4. CONCLUSION

Design and performance test of the 2 kW binary cycle geothermal power plant have been accomplished. Regarding the experimental result shown in Table 4, the important things that can be inferred from this study can be summarized as follows:

- Binary cycle power plant can be applied using relatively low enthalpy heat sources.

- The methods for designing the equipments have been proven to be accurate.

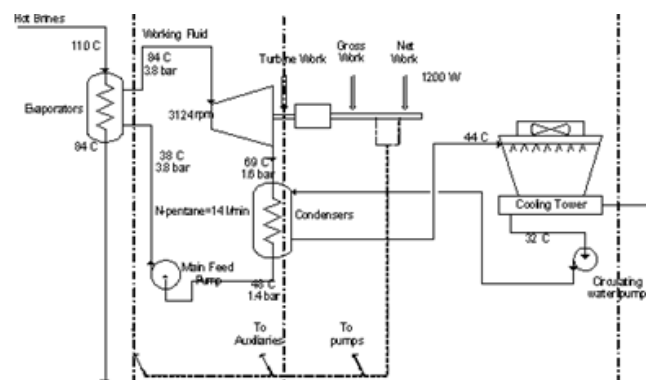**Figure 15. Assembly of 2 kW binary cycle plant at Wayang Windu**

Figure 16. Measurement location of parameters

7

Teguh et al.

Table 4. One of experimental series of measurements

Location	Unit	Design	Measurement
Inlet Evap.– Brine Temp.	℃	95	110
Outlet Evap. – Brine Temp.	℃	78.5	84
Inlet Evap. – n-Pentane Flowrate	l/min.	13.7	14
Inlet Evap. – n-Pentane Pressure	bara	3.5	3.8
Inlet Evap. – n-Pentane Temperature	℃	40.46	38
Outlet Evap.– n-Pentane Pressure	bara	3.48	3.8
Outlet Evap. – n-Pentane Temperature	℃	74	84
Inlet Cond. – n-Pentane Pressure	bara	1.36	1.6
Inlet Cond – n-Pentane Temperature	℃	62.3	69
Outlet Cond. – n-Pentane Pressure	bara	1.35	1.4
Outlet Cond. – n-Pentane Temperature	℃	41.96	48
Inlet Cond. – Cooling Water Temperature	℃	31	32
Outlet Cond. – Cooling Water Temperature	℃	37.5	44
Turbine – Rotation Velocity	rpm	3000	3124
Generator – Voltage	V	220	210
Generator – Power	W	1800	1200

REFERENCES

Bambang T. Prasetyo et all, Design and Manufacture of 2kW Binary Cycle Plant Model, Technical Report, P3TPSE-BPPT, Jakarta, 2006

Bambang T. Prasetyo et all, Design and Manufacture of 2kW N-pentane Turbine, Technical Report, P3TPSE-BPPT, Jakarta, 2006

Bambang T. Prasetyo et all, Heat Exchangers Design for BPPT 100 kW Binary Plant, Technical Report, BPPT, Jakarta, 2008

H. J. Brackenbury, D. J. Evans and D. B. Gibons, HTFS-Design Report, Harwell-National Engineering Laboratory-Chalk River Lboratories, UK, 1993

P. Shlyakhin, Steam Turbines-Theory and Design, Peace Publishers, Moscow, s.a.

R. K. Sinott, Coulson & Richardson's Chemical Engineering, Vol. 6, Revised 2nd edition, Butterworth-Heinemann, 1998

Thomas C. Elliot, Kao Chen and Robert C. Swanekamp, Standard Handbook of Powerplant Engineering, 2nd edition, Mc Graw-Hill, 1989

TEMA, 7th Edition, 1998